Supporting Information

Novel 2-naphthyl substituted zinc naphthalocyanine: synthesis, optical, electrochemical and spectroelectrochemical properties

Tatiana V. Dubinina[a,b @], Ekaterina O. Moiseeva[a], Dmitry A. Astvatsaturov [a], Nataliya E. Borisova[a,c], Pavel A. Tarakanov[b], Stanislav A. Trashin[d,e], Karolien De Wael[d,e], Larisa G.Tomilova [a,b]

a. *Department of chemistry, Lomonosov Moscow State University, 119991 Moscow, Russian Federation.*

b. Instituite of physiologically Active Compounds, Russian Academy of Science, 142432 Chernogolovka, Moscow Region, Russian Federation.

c. A.N. Nesmeyanov Institute of Organoelement Compounds Russian Academy of Science, 28 Vavilov Str. 119334 Moscow, Russian Federation

d. AXES research group, Groenenborgerlaan 171, University of Antwerp, 2020 Antwerp, Belgium.

@Corresponding author E-mail: dubinina.t.vid@gmail.com

e. Nanolab Center of Excellence, Groenenborgerlaan 171, University of Antwerp, 2020 Antwerp, Belgium.

Figure S1. ^{1}H-^{13}C HSQC spectrum of dinitrile **2** in DMSO-d_6: aromatic region (top), expanded fragment of aromatic region (bottom).

Figure S2. ^{1}H-^{13}C HMBC spectrum of dinitrile **2** in DMSO-d_6: aromatic region (top), expanded fragment of aromatic region (bottom).

Figure S3. EI mass spectrum of compound **2**.

Figure S4. MALDI-TOF mass spectrum of complex **3**, isotopic pattern for the molecular ion (inset A) and simulated MS pattern of the molecular ion (inset B).

Figure S5. FT-IR spectra of zinc complex **3** in ZnSe (A) and compound **2** in KBr (B).

Figure S6. Thermogram (TG), derivative thermogravimetric curve (DTG) and differential scanning calorimetry (DSC) (A); results of evolved gas analysis by mass-spectrometry (B-G) for complex **3**.

Figure S7. UV-Vis spectra of the solution of **3** in *o*-DCB after addition of 1vol % pyridine at various concentrations (green line - $c=1.1\times10^{-4}$, blue line – $c=6.9\times10^{-6}$, dashed lines – intermediate concentrations) (A). The molar extinction coefficient vs concentration plot (B).

Figure S8. UV-Vis (solid lines) and fluorescence (dash lines, λ_{ex} = 695 nm), spectra of solution of compound **3** diluted from $c=2.0\times10^{-5}$ M to $c=1.25\times10^{-6}$ M in *o*-DCB after the addition of 1vol% pyridine (**A**). Fluorescence quantum yield at various concentrations for the solution of compound **3** in *o*-DCB after the addition of 1vol% pyridine (**B**).

Figure S9. UV-Vis (solid lines) and fluorescence (dash lines, λ_{ex} = 695 nm), spectra of solution of compound **3** diluted from $c=2.0\times10^{-5}$ M to $c=0.625\times10^{-6}$ M in *o*-DCB after addition of 0.12 M of NBu_4F (**A**). Fluorescence quantum yield at various concentrations for the solution of compound **3** in *o*-DCB after addition of 0.12 M of NBu_4F, λ_{ex} = 695 nm (**B**).

Figure S10. EPR spectra of freshly prepared solution of compound **3** in *o*-DCB ($c=3\times10^{-5}$M) (black line) and solution after 7 days storage (blue line).

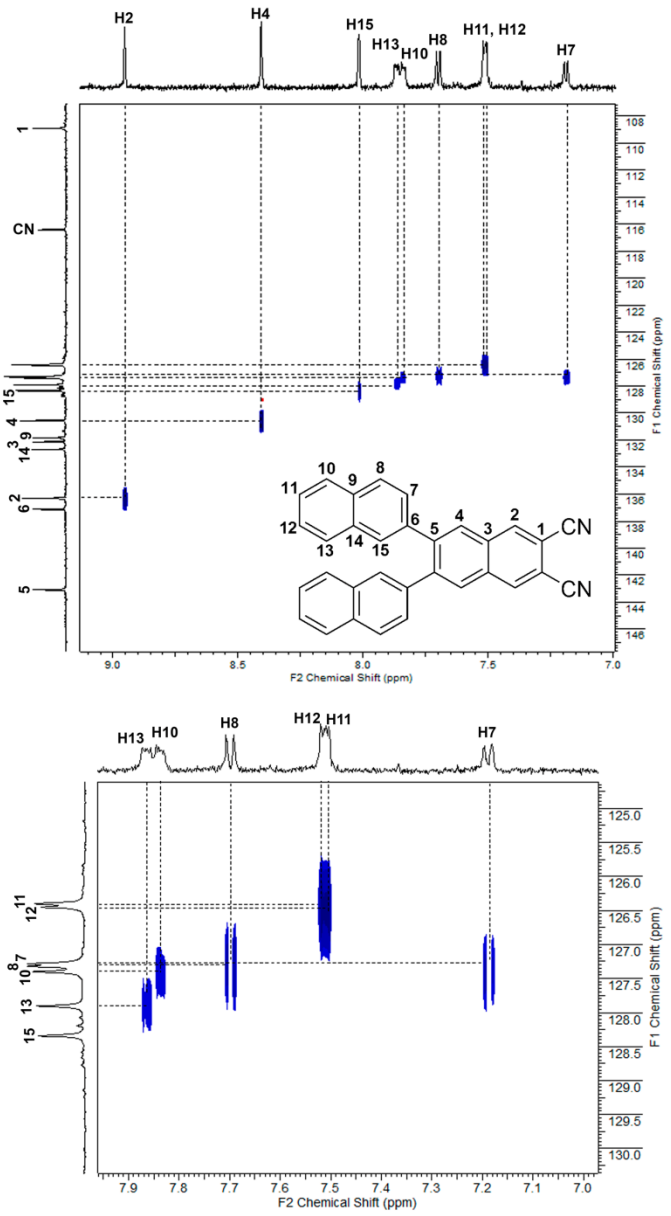

Figure S1. ^{1}H-^{13}C HSQC spectrum of dinitrile **2** in DMSO-d_6: aromatic region (top), expanded fragment of aromatic region (bottom).

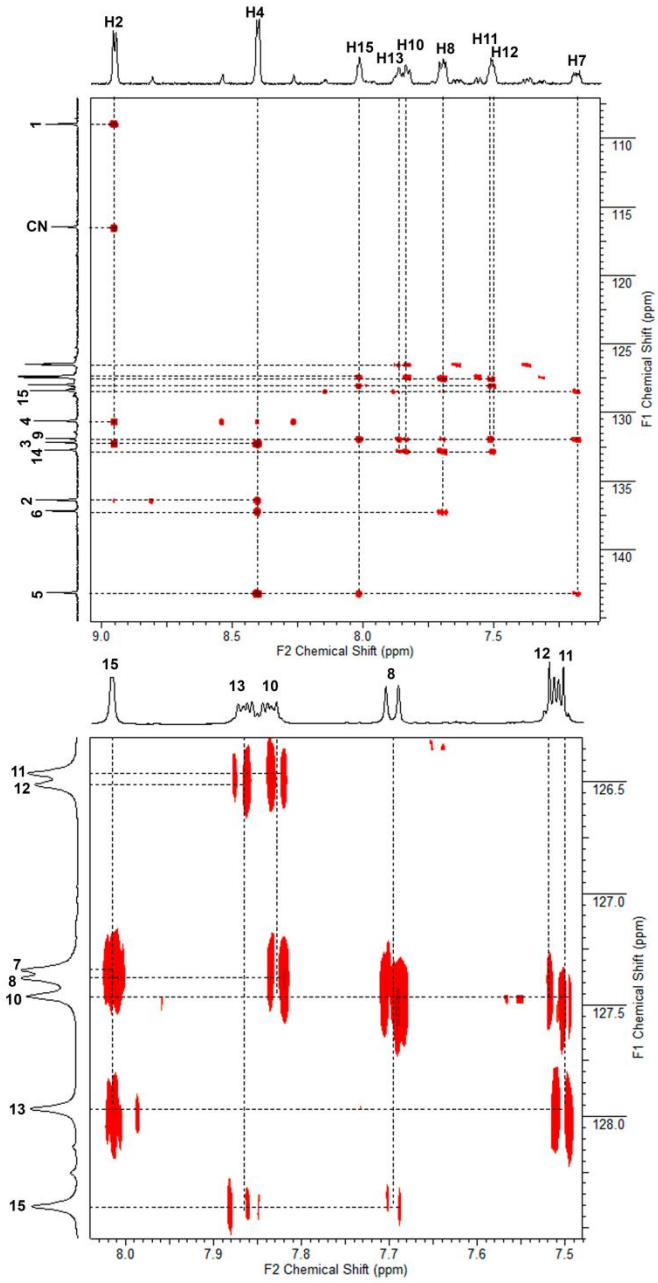

Figure S2. ^{1}H-^{13}C HMBC spectrum of dinitrile **2** in DMSO-d_6: aromatic region (top), expanded fragment of aromatic region (bottom).

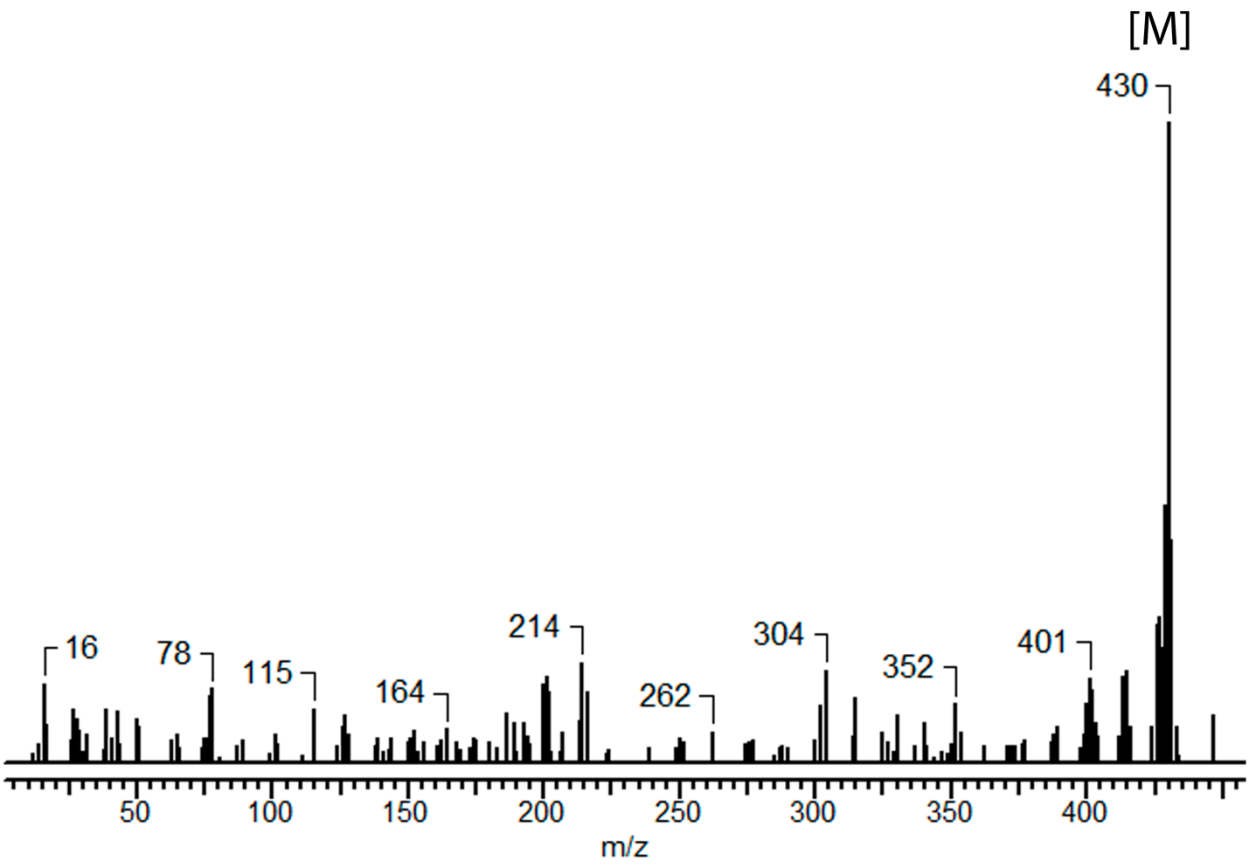

Figure S3. EI mass spectrum of compound **2**.

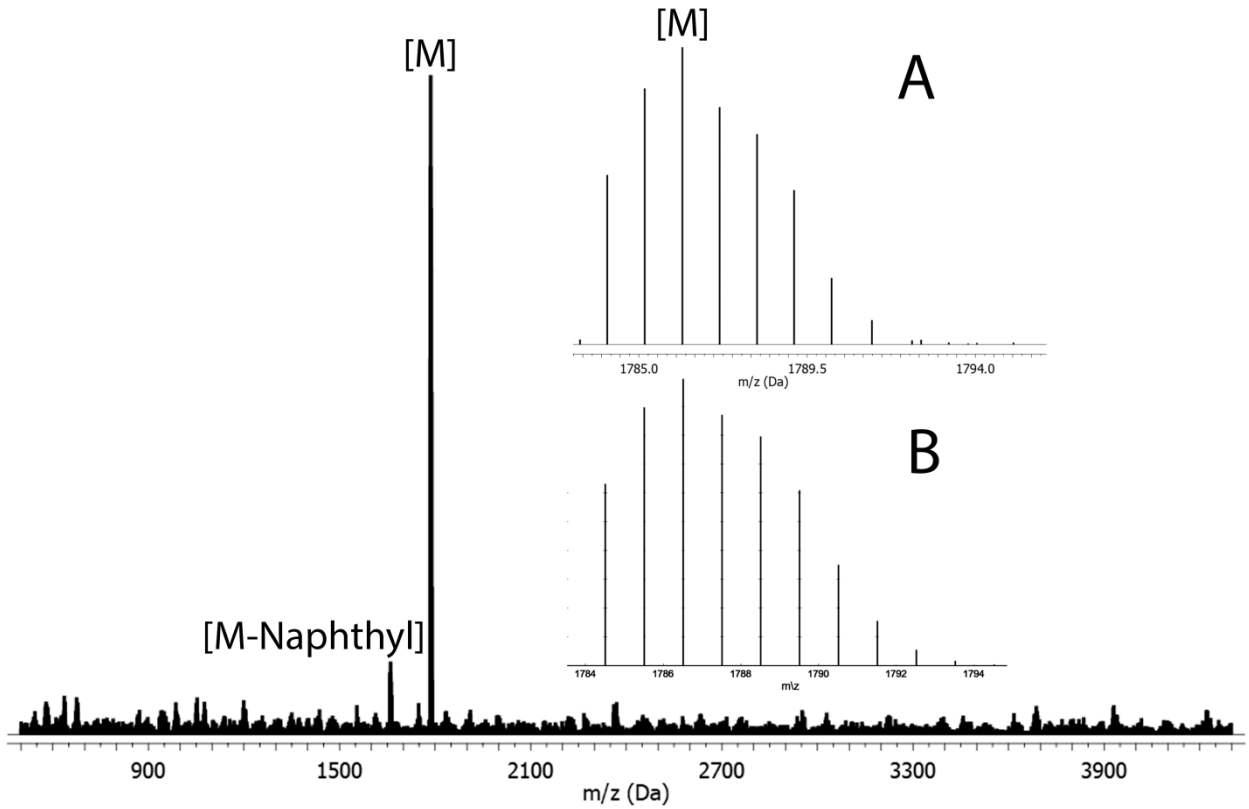

Figure S4. MALDI-TOF mass spectrum of complex **3**, isotopic pattern for the molecular ion (inset A) and simulated MS pattern of the molecular ion (inset B).

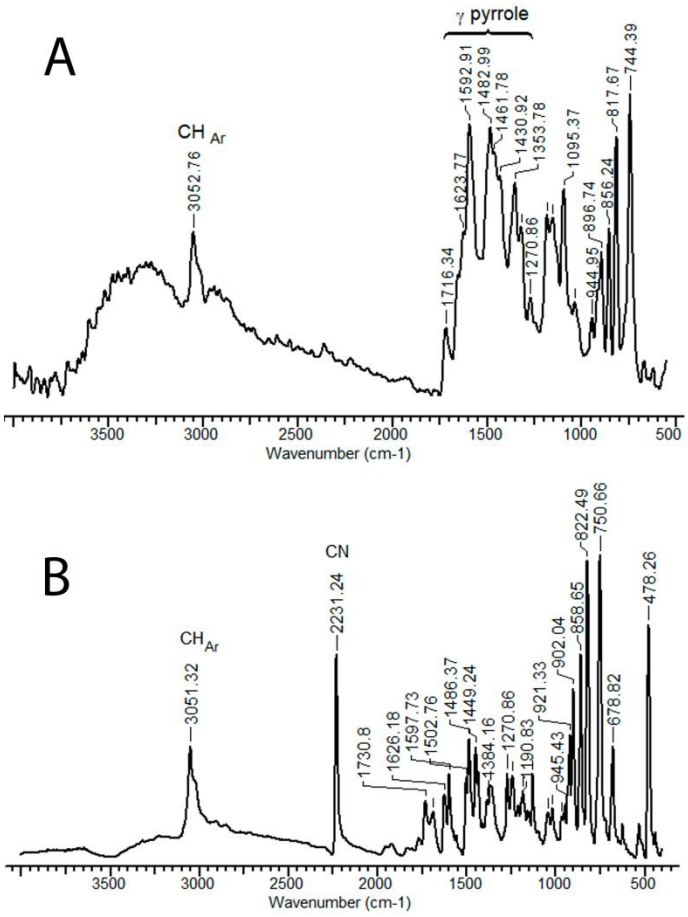

Figure S5. FT-IR spectra of zinc complex **3** in ZnSe (A) and compound **2** in KBr (B).

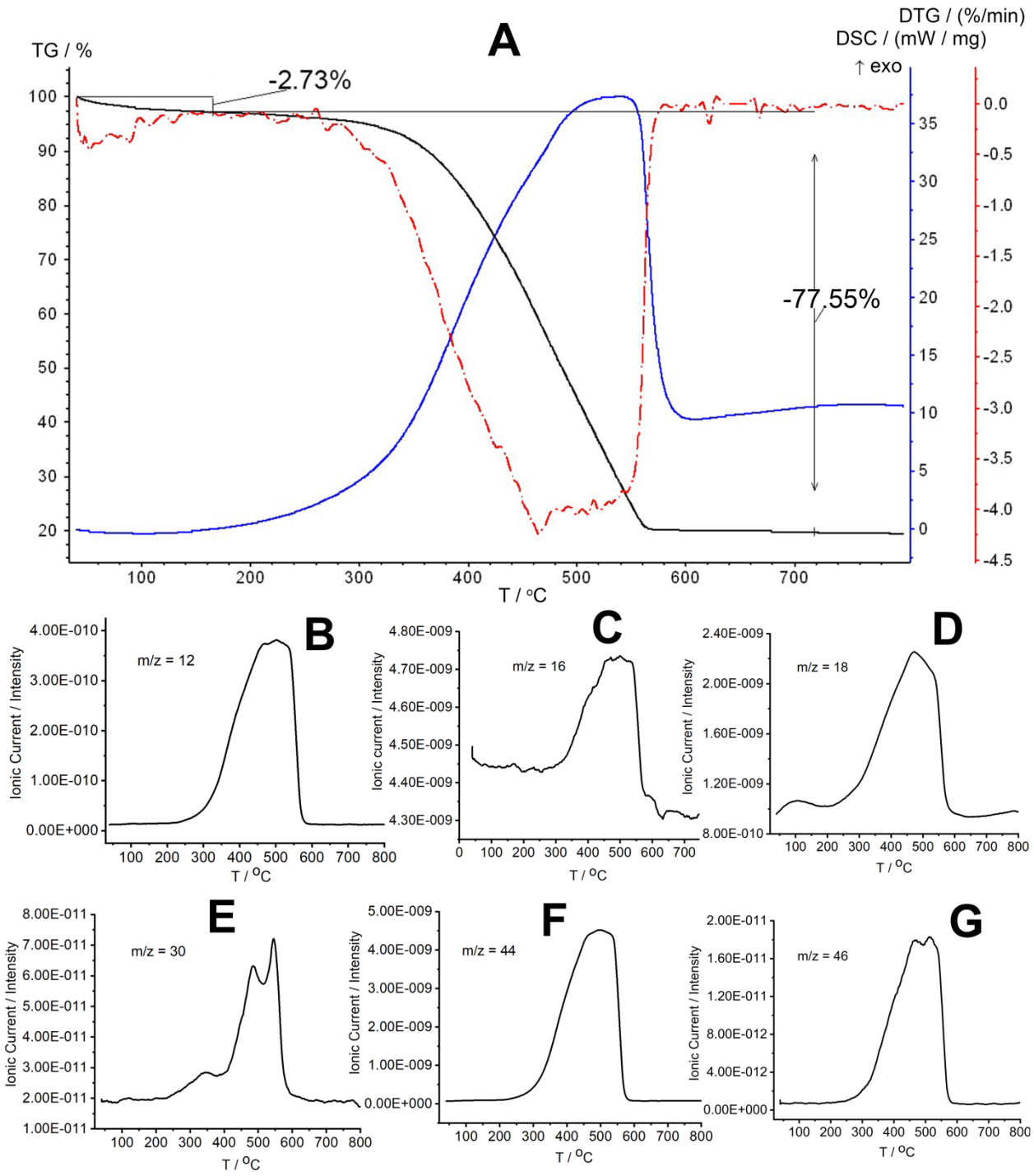

Figure S6. Thermogram (TG), derivative thermogravimetric curve (DTG) and differential scanning calorimetry (DSC) (A); results of evolved gas analysis by mass-spectrometry (B-G) for complex **3**.

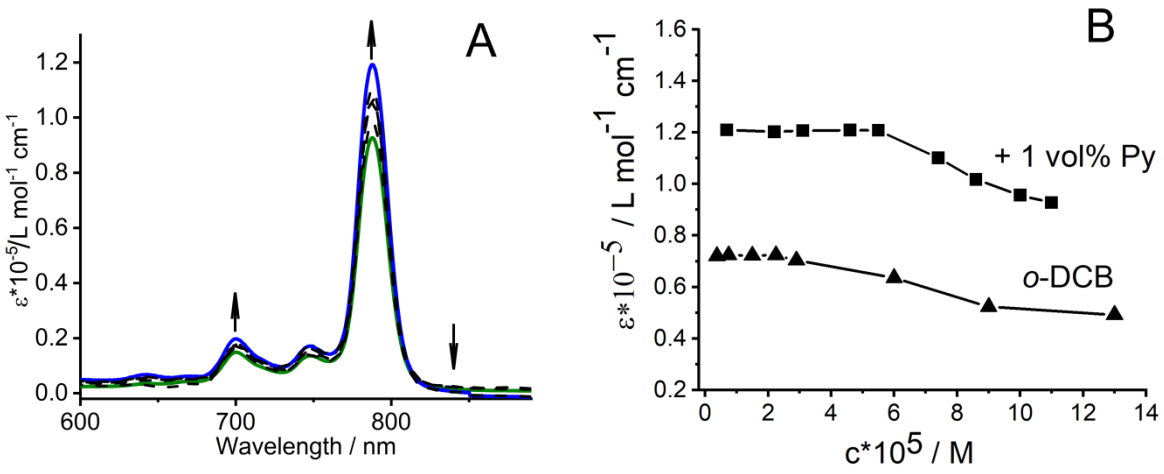

Figure S7. UV-Vis spectra of the solution of **3** in *o*-DCB after addition of 1vol % pyridine at various concentrations (green line - $c=1.1\times10^{-4}$, blue line – $c=6.9\times10^{-6}$, dashed lines – intermediate concentrations) (A). The molar extinction coefficient of *Q* band vs concentration plot (B).

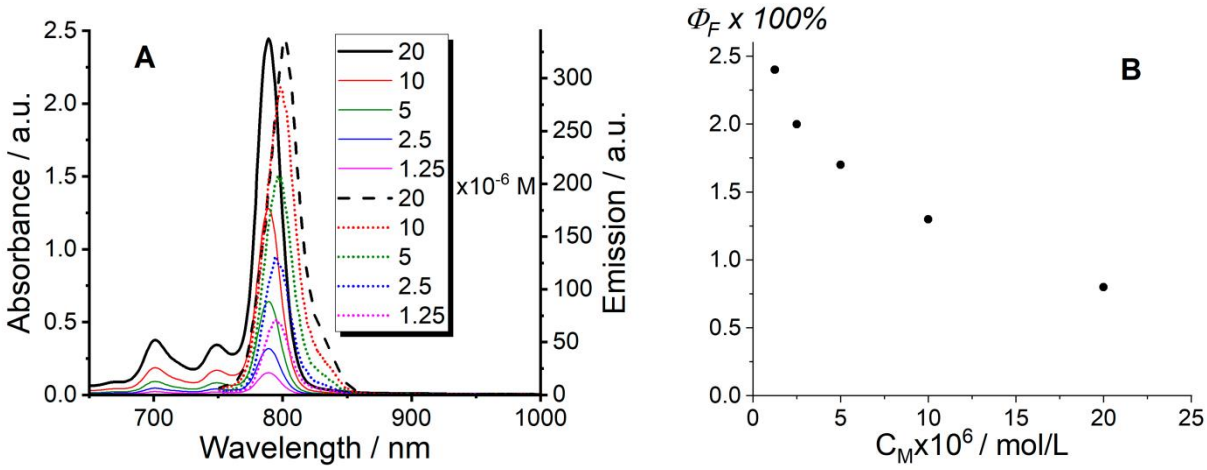

Figure S8. UV-Vis (solid lines) and fluorescence (dash lines, λ_{ex} = 695 nm), spectra of solution of compound **3** diluted from $c=2.0\times10^{-5}$ M to $c=1.25\times10^{-6}$ M in *o*-DCB after the addition of 1vol% pyridine (**A**). Fluorescence quantum yield at various concentrations for the solution of compound **3** in *o*-DCB after the addition of 1vol% pyridine (**B**).

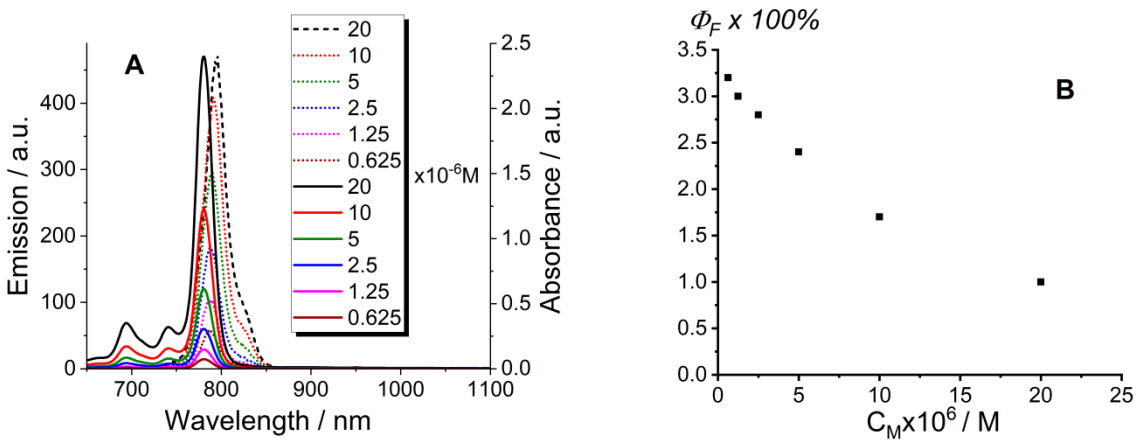

Figure S9. UV-Vis (solid lines) and fluorescence (dash lines, λ_{ex} = 695 nm), spectra of solution of compound **3** diluted from c=2.0×10^{-5} M to c=0.625×10^{-6} M in *o*-DCB after addition of 0.12 M of NBu_4F (**A**). Fluorescence quantum yield at various concentrations for the solution of compound **3** in *o*-DCB after addition of 0.12 M of NBu_4F, λ_{ex} = 695 nm (**B**).

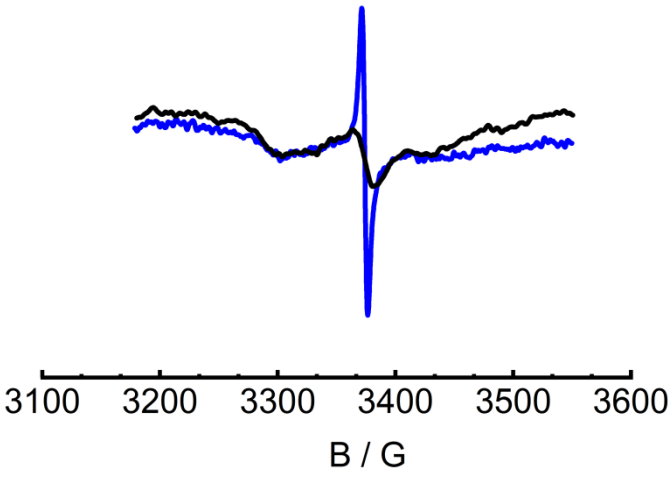

Figure S10. EPR spectra of freshly prepared solution of compound **3** in *o*-DCB (c=3×10^{-5}M) (black line) and solution after 7 days storage (blue line).